JOURNAL OF SPACECRAFT AND ROCKETS
Vol. 42, No. 3, May–June 2005

Modeling Reaction-Control-System Effects on Mars Odyssey

Jill L. Hanna Prince*
NASA Langley Research Center, Hampton, Virginia 23681
Zachary Q. Chavis†
George Washington University, Hampton, Virginia 23681
and
Richard G. Wilmoth‡
NASA Langley Research Center, Hampton, Virginia 23665

During the Mars 2001 Odyssey aerobraking mission, NASA Langley Research Center performed six-degree-of-freedom simulations to model rotational motion of the spacecraft. The main objective of this study was to assess the reaction-control-system models and their effects on the atmospheric flight of Odyssey. Based on these models, a comparison was made between data derived from flight measurements to simulated rotational motion of the spacecraft during aerobraking at Mars. The differences between the simulation and flight-derived Odyssey data were then used to adjust the model aerodynamic parameters as a result of reaction-control-system firings to achieve a better correlation.

Nomenclature

A	=	reference area, m^2
a_y	=	acceleration in y body coordinate frame, m/s^2
C_D	=	drag coefficient
C_m	=	moment coefficient
L	=	reference length, m
M_{CM}	=	moment about the center of mass
m	=	spacecraft mass, kg
q	=	dynamic pressure, N/m^2
ρ	=	atmospheric density, kg/m^3

Introduction

MARS Odyssey successfully completed the aerobraking phase of its mission in January of 2002, achieving a nearly circular orbit, and after performing minor orbit corrections project engineers began preparation for the science mapping mission. Successful aerobraking depends on numerous factors, not the least of which is maintaining a spacecraft attitude that provides optimum drag during the pass through the atmosphere. Although the Odyssey spacecraft was designed to be aerodynamically stable[1] and was expected to maintain a specific average orientation with respect to the flight path, the small aerodynamic forces and moments exerted by the tenuous atmosphere were insufficient to completely dampen any attitude oscillations induced by targeting alignment errors, atmospheric winds, residual inertial motions, etc. Therefore, an attitude control system consisting of reaction wheels and reaction-control-system (RCS) thrusters along with appropriate control logic was used to maintain the spacecraft attitude within acceptable limits. Control during the drag pass was maintained by the RCS thrusters, which were also used to desaturate the reaction wheels as necessary and to slew the spacecraft as required for solar power collecting and communications during the nonaerobraking portion of the orbit.

RCS thrusters firing in a vacuum or in the low-density Mars atmosphere encountered by Odyssey produce plumes that expand rapidly and can impinge on other parts of the spacecraft as well as interact with the flow around the spacecraft during aerobraking. These plumes can produce effects on the aerodynamic control effectiveness. Impingement effects were discovered during the termination phase of Magellan.[2] Analyses performed for Mars Global Surveyor (MGS) showed that certain thruster firings at the higher densities expected for MGS aerobraking could actually produce thrust reversing.[3] However, the Odyssey RCS thrusters were considerably smaller than those used on MGS, and such effects were expected to be small.

Furthermore, the physical arrangement of the Odyssey RCS thrusters is such that the principle thrust directions are nearly perpendicular to the flight direction (see Fig. 1), and any interactions with the flow around the spacecraft would be considerably different than for MGS. Therefore, preflight analyses were conducted using a simple engineering plume model[4] coupled with flow simulations using the direct simulation Monte Carlo (DSMC) method[5] to assess the magnitude of both impingement and plume-induced flow interaction effects on Odyssey aerodynamics. The results from these simulations were used to augment the aerodynamic database already developed[1] to extract atmospheric densities from accelerometer data and for other trajectory simulations used in various mission support tasks. These aerodynamic databases both with and without RCS thruster effects were then used in six-degree-of-freedom (DOF) simulations to assess the RCS model by comparisons to flight data.

This paper provides a brief description of the RCS plume model and the DSMC simulations used for flowfield and aerodynamic predictions. The effects of firing various RCS thrusters will be presented for Odyssey aerobraking conditions, and the incorporation of the predicted increments in forces and moments into six-DOF simulations will be discussed. Finally, comparisons of the six-DOF predictions with flight data will be provided for selected aerobraking passes.

ACS Description

The attitude-control-system (ACS) control frame for Odyssey is composed of two star cameras, two sun sensors, two local inertial measurement units (IMU), two sets of two-axis gimbals, the RCS, and four reaction wheels.[6] The IMUs contain the accelerometers from which atmospheric density is derived by using Eq. (1):

$$a_y = \rho(C_D A/2m) \tag{1}$$

This density profile is input to the Program to Optimize Simulated Trajectories (POST) six-DOF simulation. The reaction-wheel

Received 30 December 2002; accepted for publication 4 November 2004. This material is declared a work of the U.S. Government and is not subject to copyright protection in the United States. Copies of this paper may be made for personal or internal use, on condition that the copier pay the $10.00 per-copy fee to the Copyright Clearance Center, Inc., 222 Rosewood Drive, Danvers, MA 01923; include the code 0022-4650/05 $10.00 in correspondence with the CCC.

*Aerospace Engineer, Vehicle Analysis Branch, MS 365. Member AIAA.
†Graduate Research Scholar Assistant. Student Member AIAA.
‡Research Scientist, Aerothermodynamics Branch, MS 408A. Senior Member AIAA.

Table 1 RCS firings that control individual axis rotations

Axis	RCS-1	RCS-2	RCS-3	RCS-4
$+x$	On	Off	Off	On
$-x$	Off	On	On	Off
$+y$	On	On	Off	Off
$-y$	Off	Off	On	On
$+z$	On	Off	On	Off
$-z$	Off	On	Off	On

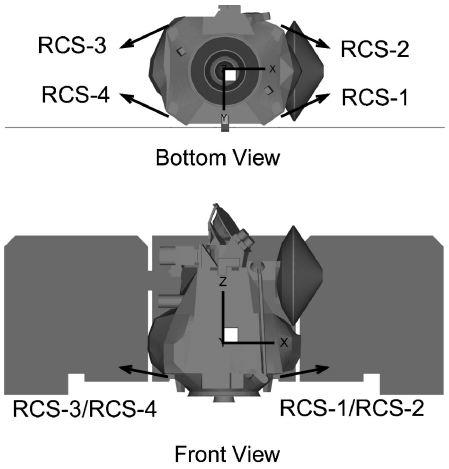

Fig. 1 Sketch of Odyssey spacecraft showing RCS locations and thrust vectors.

desaturation profile is also input to six-DOF POST. The remaining components of the ACS are not considered here because their influence was expected to be small.

Reaction-Wheel Model

The Mars Odyssey ACS contained four reaction wheels: three arranged along orthogonal axes and one skew, offset in the assembly frame so that equal torque is achieved in the x, y, and z spacecraft coordinate frame.[6] The reaction wheels were modeled in six-DOF POST. Telemetry received from the Odyssey spacecraft reported reaction-wheel speeds. With the knowledge of reaction-wheel gains and inertias, the reaction-wheel speeds were converted to a net reaction-wheel torque and summed into the environmental moments.

Plume Aerodynamic Model

The Odyssey RCS consists of four monopropellant hydrazine thrusters located as shown in Fig. 1. These thrusters have a nominal thrust of 0.88 N, and their axes are canted such that they can be fired in various combinations to provide three-axis attitude control (Table 1).

Outside the atmosphere, the thruster plumes expand rapidly and can produce impingement primarily on the backside of the solar panels. During aerobraking, the plumes can also interact with the flow around the spacecraft thereby altering the aerodynamics. Both of these conditions produce incremental forces and moments on the spacecraft in addition to those produced by the thrust of the nozzles themselves that must be taken into account for accurate attitude modeling. A complete analysis of these RCS aerodynamic effects requires modeling of the flow inside the thruster, the flow in the plume, and the resulting flow around the spacecraft. Because the latter effects depend on both the aerodynamic (relative wind) attitude of the spacecraft and the atmospheric density, the ultimate product of these analyses is an RCS aerodynamic database that can provide these incremental forces and moments throughout the aerobraking pass, that is, as a function of attitude and density.

Plume-Flow Model

The internal nozzle flow was computed using a Navier–Stokes solver[7] to provide the exit plane properties. The computations started upstream of the throat by using the stagnation chamber pressure of 2.034 MPa and temperature of 1167 K. The geometry upstream of the throat was approximated to provide a smooth convergent section; the throat diameter was 0.29 cm, and the divergent section was a 15-deg half-angle cone with an exit-to-throat area ratio of 100. The internal flow was assumed to be laminar, and the gas was modeled as a perfect gas.

The plume-flow model used in the present study was devised by Woronowicz and Rault[7] and adapted for Odyssey by Chavis and Wilmoth.[4] The model is used to compute properties in the plume based on source-flow principles and derived from a free-molecular formulation of conservation of mass, momentum, and energy. The derivation assumes that the flow expands radially from each of a distribution of point sources whose properties are specified based on the exit plane solution just described. Although the free-molecular description of the flow is not valid in the continuum core of the plume and the source-flow assumption breaks down near the nozzle exit, it has been found that the radial expansion assumption gives a reasonably accurate approximation of the spatial variations in plume-flow properties at sufficiently large distances from the exit. Furthermore, this model has been shown to capture much of the functional dependence of these properties on nozzle-exit conditions[7] and to produce far-field plume properties that are comparable to those predicted by full Navier–Stokes computations.[4]

DSMC Flow Simulations

The impingement of the plume on nearby spacecraft surfaces and the flow around the spacecraft was modeled by using the DSMC method.[5] The DSMC computations were performed by using the DSMC Analysis Code (DAC) of LeBeau and Lumpkin,[8] which was also used separately to compute the basic aerodynamics of Odyssey.[1] DSMC models the molecular nature of low-density flows by tracking the motion and collisions of millions of individual molecules. These flows typically are not in thermodynamic equilibrium and cannot be modeled with conventional continuum methods. Macroscopic properties within the flow and forces and moments on surfaces within the flow domain are determined by statistical sampling. DAC can treat complex three-dimensional geometries and allows nonuniform inflow boundaries to be defined to simulate plumes or other inflows whose properties must be defined by other means.

The plume effects were introduced into the DSMC computations by defining an isodensity boundary from the plume-source-flow solution to approximate the boundary between continuum and transitional flow. Although this boundary is more commonly chosen based on breakdown criteria established by Bird,[5] these criteria are typically based on local density gradients, which are not accurately captured with simple source-flow solutions. Therefore, the isodensity condition was chosen for these studies based on a ratio of the local-to-freestream momentum flux of 100, which allows the DSMC solution to capture the bulk of the interaction of the plume and freestream flows. A typical isodensity boundary surface for Odyssey is shown in Fig. 2. Because each of the Odyssey RCS thrusters have identical nozzle and plume characteristics, this surface is constructed such that it can be translated and rotated to represent any of the four thrusters. For multiple thruster firings, multiple surfaces are used. The location and size of these surfaces is such that these surfaces do not overlap, so that any plume–plume interactions are fully captured by the DSMC computations.

Flow Simulation and Aerodynamic Results

Figure 3 shows surface contours from a typical DSMC solution, which illustrate both the directed flux onto the spacecraft from the expanding plume and the resulting pressure contours on the surface for a typical aerobraking condition. The thrusters designated RCS-2 and RCS-3 produced the largest direct impingement effects on the solar panel even though they were further away than RCS-1 and RCS-4 because the thrust axes of RCS-2 and RCS-3 were canted toward the panel. However, these impingement effects are not as

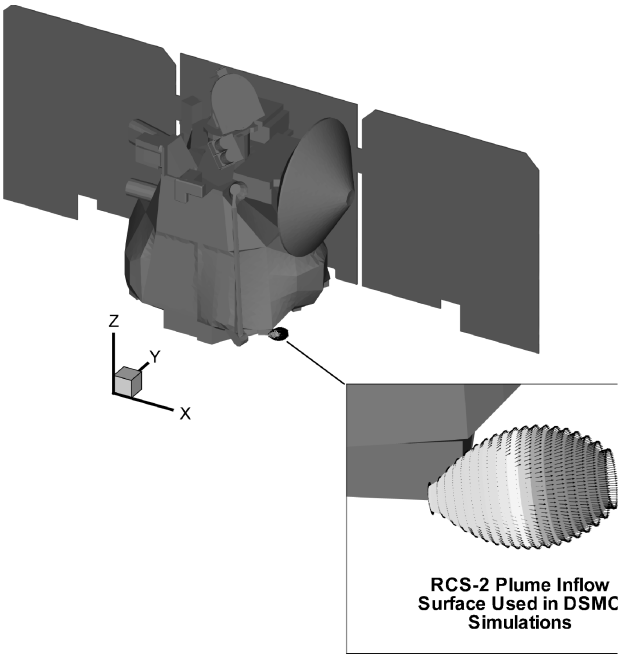

Fig. 2 Plume inflow model used in DSMC simulations of plume impingement and plume–freestream interactions.

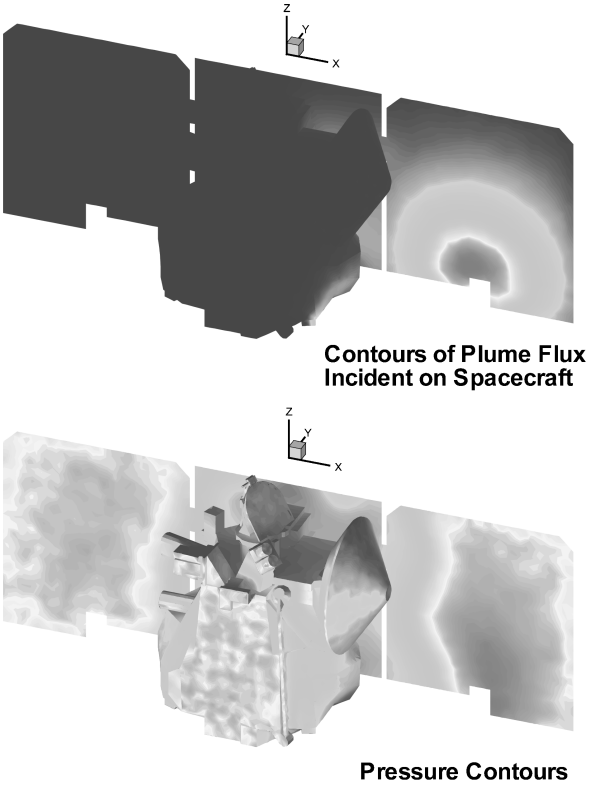

Fig. 3 Plume impingement flux and pressure contours for RCS-2 firing during aerobraking: atmospheric density = 100 kg/km^3 and spacecraft attitude at zero pitch and yaw.

clearly evident in the pressure contours of Fig. 3 because the atmospheric flow around the spacecraft during aerobraking interacts with the plume causing the impingement effects to be diffused. The plume also tends to act as a shield, which blocks the atmospheric molecules from reaching the panel surface, so that the net effect on the aerodynamics is quite complex.

DSMC simulations were performed with and without RCS firings for various combinations of thrusters, various densities (including zero to capture direct impingement effects in the absence of the atmosphere), and various spacecraft attitudes. The aerodynamic forces and moments from these simulations were then used to construct a database that provided the increments in forces and moments that were needed to perform the six-DOF simulations. A typical set of increments in moment coefficients about the spacecraft mechanical axes is shown in Fig. 4 for RCS-1 and RCS-2. These increments do not include the contribution from the actual RCS thrust forces but only those caused by impingement and aerodynamic flow interaction. Because these increments are shown here as coefficients ($C_m = M_{\mathrm{CM}}/qAL$), their values are singular as the density approaches zero. However, in the implementation of the database, the zero-density increments are replaced by dimensional quantities that represent the vacuum impingement effects only.

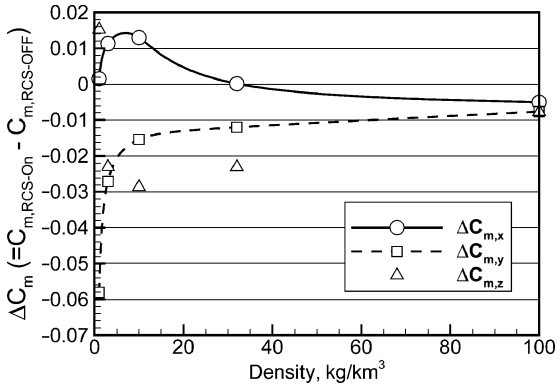

a) RCS-1

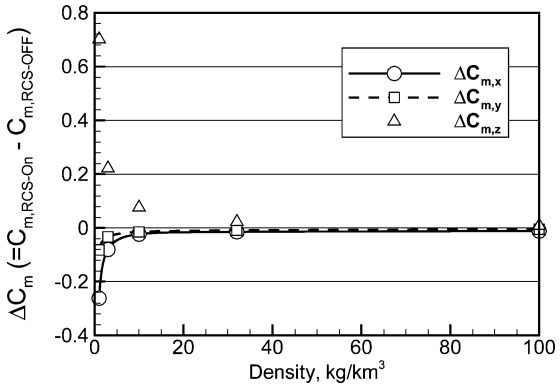

b) RCS-2

Fig. 4 Increments in aerodynamic moments produced by various thruster firings: spacecraft attitude at zero pitch and yaw.

The results shown here represent only a small part of the computations required to construct the database used for six-DOF simulations. Further details of the computations and results are provided in Ref. 4.

Six-DOF Models

Initial inputs to POST six-DOF were defined at a given time before periapsis passage. Depending on the duration of the drag pass, this time ranged from 600–400 s before the time of periapsis. Inputs to the simulation were time, spacecraft position, velocity, orientation, angular rates, and reaction-wheel speeds. Profiles of density and reaction-wheel speeds throughout the drag pass were also included in the simulation.

Orientation, angular rates, thruster on-times, and reaction-wheel speeds were obtained through spacecraft telemetry. Spacecraft position and velocity were acquired by Jet Propulsion Laboratory. Thruster on-times were obtained from small forces files (SFF) generated onboard the spacecraft. The SFF provide cumulative effects of delta-V over a specific time interval.[9] During Odyssey operations, this time interval was set to ±600 s from periapsis to incorporate any possible RCS thruster firings within the atmosphere.

Density profiles were 7-s running means of the density obtained through accelerometer measurements analyzed by the George

Washington University accelerometer team at NASA Langley Research Center. A 7-s average was used to reduce noise within the density profile while still including density spikes or abnormalities within the atmosphere.[10]

Six-DOF Results

The six-DOF POST was used during the aerobraking phase operations at NASA Langley Research Center to validate or adjust the aerodynamics subroutine. Comparisons of body angular rates and Euler angles were available for every orbit, and any trends in substandard comparisons would possibly lead to changes or corrections in the aerodynamics subroutines. Validations of the six-DOF POST were performed on several preaerobraking exoatmospheric situations to ensure that proper implementation of the nonaerodynamic models in POST were correct. These situations included the second trajectory correction maneuver (TCM) on 20 June 2001 and several orbit passes around Mars before Odyssey first skimmed the Mars atmosphere.

TCM2 Validation

During the cruise phase of the Odyssey mission, there were four scheduled TCM burns to correct trajectory dispersions in preparation for insertion into orbit around Mars. During the second of these burns designed as an optimization strategy to minimize total required propellent, data were received at NASA Langley to validate the RCS and reaction-wheel models in the six-DOF simulation. These data thruster accumulated pulses, quaternions, angular rates, and reaction-wheel speeds. From these data, a profile of Euler angles and angular rates were simulated by using the six-DOF POST.

Figure 5 shows 400 s of the TCM during which there were few or no RCS thruster firings. If there were thrusters fired in this time period, they were fired for shorter than 0.1 s and did not record on the telemetry report. This comparison was made to validate the implementation of the reaction-wheel model. There were slight variations in the reaction-wheel speeds that corresponded to slight variations in the angular rates of Odyssey. Most of the high-frequency oscillations in the flight data are attributed to IMU noise. The rates center about zero with no peaks greater than 0.025 deg/s. The six-DOF POST captured the slight changes in rates and therefore validated this aspect of the simulation.

Figure 6 shows a separate phase of TCM2 during which there were several firings of the RCS thrusters. These firings are from RCS-1 and RCS-2 and are most prevalent in the roll rate, resembling steep almost instantaneous decreases in rate. The six-DOF POST captures these firings at the correct time, but there is a small overshoot in the thrust that accumulates with time. The thrusters did not produce as much thrust as was simulated, posing the possibility of thruster impingement effects upon the solar arrays that had not been previously modeled. Although the possibility of thruster impingement had been examined at the time of this validation, the RCS

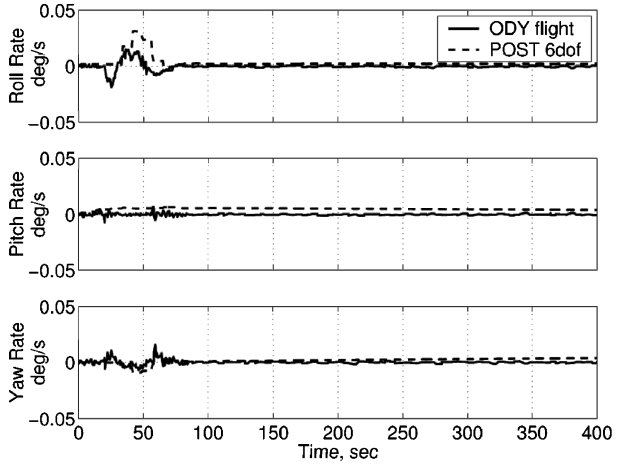

Fig. 5 TCM2 validation, no RCS firing: Odyssey body angular rates.

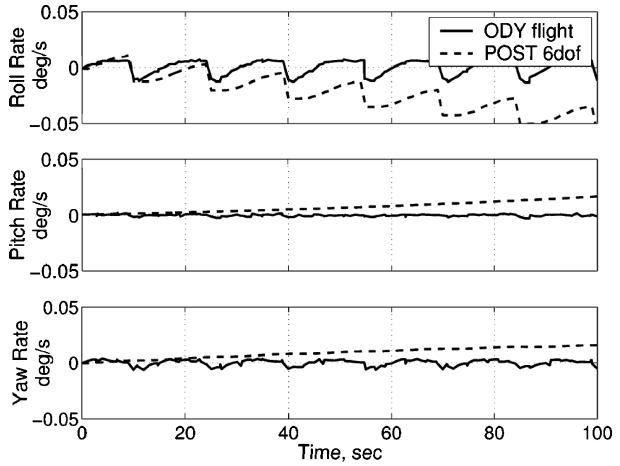

Fig. 6 TCM2 validation with RCS firing: Odyssey body angular rates.

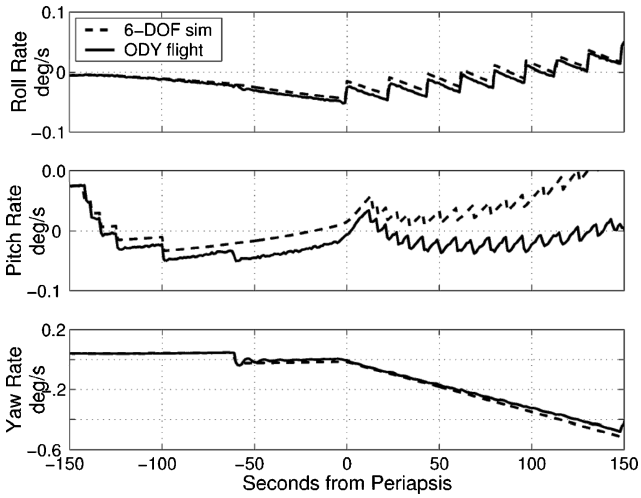

Fig. 7 Periapsis 4 body angular rates.

impingement model was not used in this validation. Because of the thrust overshoot after approximately 20 s, the pitch rate and yaw rate also deviate slightly from the flight data. Nevertheless, this test validates the correct implementation of the thruster model without impingement effects.

Exoatmospheric Orbit Validation

The first orbital passes of Odyssey around Mars provided for exoatmospheric orbital data analysis to again validate models that did not depend on atmospheric density. Periapsis altitudes before orbit pass 8 were higher than 150 km above the reference ellipsoid of Mars, so that the six-DOF POST was run assuming flight in a vacuum.

Figure 7 shows Odyssey angular rates 150 s before and after periapsis 4. The roll rate captures all of the thruster firings in this time interval. The vast majority of all thruster firings during Odyssey aerobraking were from RCS-1 and RCS-2 to control the roll rate of the spacecraft (see Table 1). The angular roll-rate comparison is good to within 0.001 deg/s. The yaw rate also compares extremely well, simulating the flight data to within 0.05 deg/s. The pitch rate in POST resembles the same pattern as the flight data with the exception of one point at approximately 65 s before periapsis, where there is a sharp decrease in pitch rate that the simulation does not capture. This is either a thruster firing that the small forces file did not report or more probably, a coupling among the axes that the simulation did not model. Note that the simulation detected the decrease in flight yaw rate at approximately 60 s before periapsis, but the simulation did not detect any coupling to the pitch rate indicated in the flight data at the same time. If the simulation had followed the flight data at this point, the pitch rate would have matched better throughout this test.

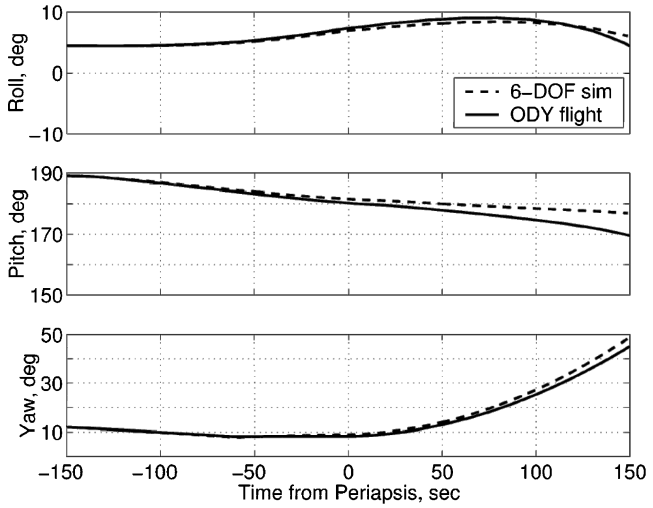

Fig. 8 Periapsis 4 Euler angles.

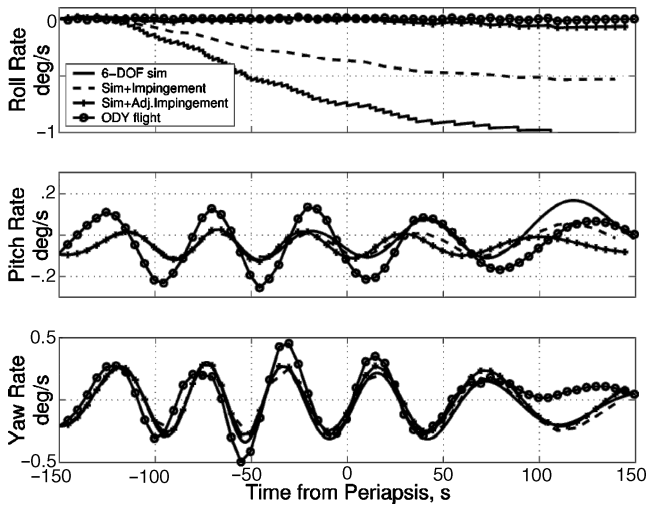

Fig. 9 Periapsis 161 body angular rates.

Figure 8 shows the spacecraft roll, pitch, and yaw from the same periapsis. As expected, because the simulation of body angular rates and the flight data are so comparable, the Euler angles are similarly close; the roll and yaw angles are within 2 deg of the flight data after 300 s of simulation, and the pitch angle is within 8 deg after the same time period. Note that this larger discrepancy is again caused by the missed decrease in pitch rate at approximately 65 s before periapsis.

Aerobraking Results

Once Odyssey entered the Mars atmosphere, the RCS impingement model was implemented into six-DOF POST. Using this model, comparisons of angular rates and roll, pitch, and yaw were generated for every orbit during Odyssey operations. The effect of the RCS impingement model is shown in Figs. 9 and 10 for periapsis 161. The dotted line indicates the Odyssey flight data. The solid line indicates the six-DOF POST without the RCS impingement model. The dashed line indicates the six-DOF POST with the implementation of the RCS impingement model. The maximum density of the 7-s running mean of density for this orbit was 49.8 kg/km^3, a typical maximum density approached by Odyssey. The discontinuities in the red line indicate RCS thruster firings simulated in six-DOF POST without the thruster impingement model. As in every orbit during aerobraking, the thruster firings appear mostly in the roll rate. The accumulated thrust overshoot in the simulation reaches 1 deg/s after 100 s. When the thruster impingement model is added to the simulation, this error decreases by 50% within the same time frame. To correct this error further, a multiplier was incorporated into the

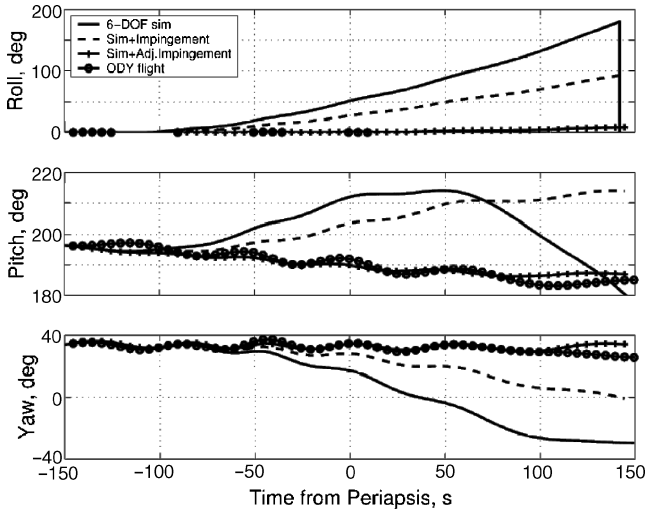

Fig. 10 Periapsis 161 Euler angles.

roll-moment coefficient within the impingement model only. Note that although RCS-2 and RCS-3 produced the most impingement effects on the spacecraft, RCS-1 and RCS-2 were fired more frequently to control the roll rate, and therefore only a roll-moment multiplier was necessary.

The multiplier for orbit 161 increased the impingement roll moment by a factor of 2.35. By decreasing the total thrust effect, the roll rate was brought closer to the actual flight data. In Fig. 9 this adjusted impingement is indicated by the green + line that is comparable to the blue line indicating the flight data. As noted in the lower plots of Fig. 9, this adjustment in the impingement model did not much affect the pitch rate or yaw rate. The simulated yaw rate shows good agreement to the flight data. Although the pitch-rate simulation does not correlate as well with the flight data, the frequency of the pitch-rate oscillations is similar to flight.

Figure 10 shows the roll, pitch, and yaw from the same orbit 161. Again, the red line of the POST simulation without the impingement model does not correlate well with the flight data. After the impingement model is added, this error decreases, but it is not until the inclusion of the 2.35 multiplier that the simulation compares to within a few degrees.

The inclusion of a multiplier on the roll-moment coefficient of the RCS impingement model was introduced during Odyssey aerobraking operations on orbit 46 to adjust the simulation to better correlate to flight data. In time, a trend developed in the magnitude of this multiplier. Figure 11 shows the variation of roll-moment multiplier with maximum density of each orbit since periapsis 46. As shown, the multiplier decreases as maximum density increases.

During Odyssey aerobraking, as a general rule, the larger density profiles required more thruster firings to stay within the desired orientation deadband. Figure 12 shows the on-times for each RCS thruster as a function of maximum density. RCS thrusters 1 and 2 fired most often, producing a negative roll about the spacecraft. As the spacecraft flew through denser regimes of the Mars atmosphere, the RCS-1 and RCS-2 fired more often to keep the roll angle under control. At higher densities, the direct impingement of the RCS thruster plumes onto the solar panel has a less significant impact than that of the thruster plume interaction with the atmospheric flow about the spacecraft (which effectively alters the vehicle aerodynamics). At lower densities, direct plume impingement is the dominant component of RCS interactions because the atmospheric flow densities are much lower than the thruster plume densities. From Fig. 11, it can be inferred that because a larger multiplier on the roll-moment coefficient was required at lower densities, the RCS impingement component was modeled less accurately than the thruster plume-atmospheric flow interaction component. At the higher densities, a smaller multiplier was required because in these regions the plume-flow interaction component was more significant than that caused by direct plume impingement.

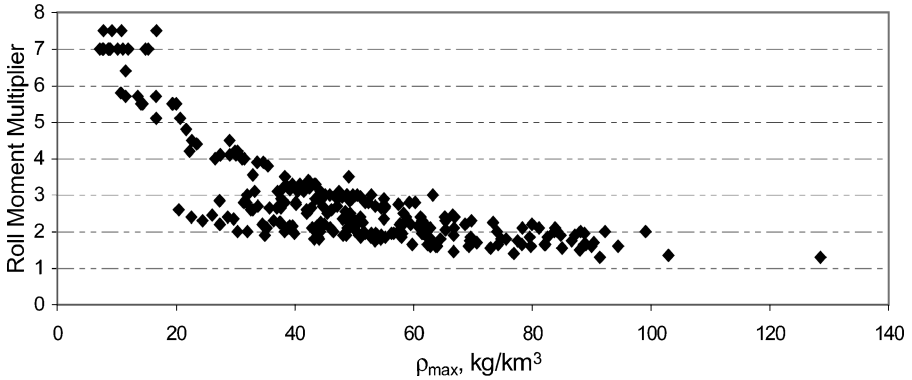

Fig. 11 Variation of roll-moment multiplier with maximum density after periapsis 46.

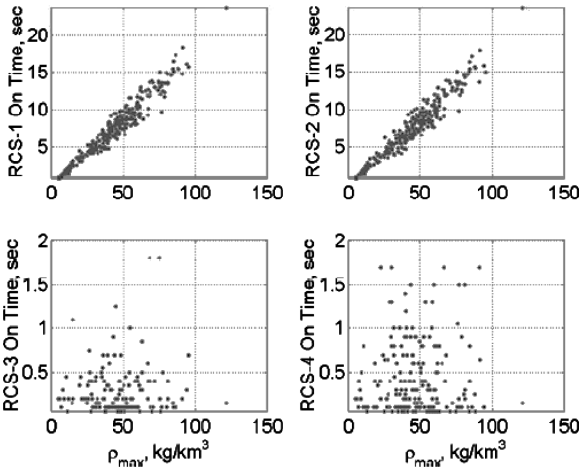

Fig. 12 Variation of RCS on-times with maximum density after periapsis 46.

Conclusions

The 2001 Mars Odyssey successfully completed its aerobraking phase with the use of reaction-control-system (RCS) thrusters to maintain attitude control within the Mars atmosphere. Several attitude control models including reaction-wheel and thruster-plume models were incorporated into a six-degree-of-freedom (DOF) simulation to accurately simulate the rotational motion of the spacecraft during flight. Upon inspection of the thruster orientation and plume effects, impingement on the solar array and interaction with atmospheric molecules reduced the effectivity of the RCS thrusters. The six-DOF analysis supported the research that was performed preflight, and with the use of adjustments to the RCS impingement model an accurate simulation of Odyssey atmospheric flight was performed.

Acknowledgment

This research was supported by NASA under Contract NAS1-97046 while the senior author was in residence at ICASE, NASA Langley Research Center.

References

[1]Takashima, N., and Wilmoth, R. G., "Aerodynamics of Mars Odyssey," AIAA Paper 2002-4809, Aug. 2002.

[2]Cestaro, F. J., and Tolson, R. H., "Magellan Aerodynamic Characteristics During the Termination Experiment Including Thruster Plume-Free Stream Interactions," NASA CR-1998-206940, March 1998.

[3]Rault, D. F., "RCS Plume Effect on Spacecraft Aerodynamics During Aerobraking Maneuver," *Rarefied Gas Dynamics 20*, edited by C. Shen, Peking Univ. Press, Beijing, 1996, pp. 549–554.

[4]Chavis, Z. Q., and Wilmoth, R. G., "Plume Modeling and Application to Mars 2001 Odyssey Aerobraking," AIAA Paper 2002-2896, June 2002.

[5]Bird, G. A., *Molecular Gas Dynamics and the Direct Simulation of Gas Flows*, Clarendon, Oxford, 1994.

[6]"Mars Surveyor Program '01—Orbiter ACS Hardware Coordinate Frame Definitions and Transformations, Algorithm: LIB-6," Rev. 7, 5 Feb. 2001.

[7]Woronowicz, M. S., and Rault, D. F. G., "On Plume Flowfield Analysis and Simulation Techniques," AIAA Paper 94-2048, June 1994.

[8]LeBeau, G. J., and Lumpkin, F. E., III, "Application Highlights of the DSMC Analysis Code (DAC) Software for Simulating Rarefied Flows," *Computer Methods in Applied Mechanics and Engineering*, Vol. 191, No. 6–7, 2001, pp. 595–609.

[9]"Software Interface Specification Small Forces File for Mars Polar Lander, Stardust, Genesis and Mars Odyssey 2001 Orbiter," Ver. 1.7, C. Acton Navigation and Ancillary Information Facility, 24 Feb. 2001.

[10]Tolson, R. H., Dwyer, A. M., Hanna, J. L., Keating, G. M., George, B. E., Escalera, P. E., and Werner, M. R., "Application of Accelerometer Data to Mars Odyssey Aerobraking and Atmospheric Modeling," *Journal of Spacecraft and Rockets*, Vol. 42, No. 3, 2005, pp. 435–443.

R. Mase
Guest Editor